Mixing and Available Potential Energy in a Boussinesq Ocean*

RUI XIN HUANG

Department of Physical Oceanography, Woods Hole Oceanographic Institution, Woods Hole, Massachussetts

(Manuscript received 18 February 1997, in final form 23 July 1997)

ABSTRACT

The commonly used definitions for available potential energy and its sources in the oceans are based on the quasigeostrophic approximation, so they are not suitable for the study of basin-scale circulation. Accurate definitions for the available potential energy and its sources and sinks can be derived from the classic definition of available potential energy. Application of the exact definitions to the ocean reveals the dynamic role of internal mixing and surface thermal forcing. It is shown that the mechanical energy required for sustaining the basic stratification by mixing light water downward plays a vitally important role in the balance of potential energy and available potential energy.

1. Introduction

According to the classic definition, available potential energy (APE) is the difference in potential energy between the physical state and the reference state:

$$E_a = E_p - E_r = g \iiint_V \rho z \, dv - g \iiint_V \rho_r Z \, dv, \tag{1}$$

where (ρ, z) and (ρ_r, Z) are the density and the vertical coordinates in the physical and reference states. In this study we will neglect the effects of pressure and salinity on density, so $\rho_r = \rho$ for the following discussion. The reference state is defined as the state of minimum potential energy that can be reached through reversible adiabatic processes. In the reference state, all density surfaces are level. For an ocean with flat bottom, the vertical height in the reference state, $Z = Z(\rho)$, can be determined by either a computer-sorting program, which reorganizes the vertical position of layers in the reference state according to their density, or in terms of

$$Z(\rho(\mathbf{x}, t)) = \frac{1}{A} \iiint_V H(\rho(\mathbf{x}', t) - \rho(\mathbf{x}, t)) \, d\mathbf{x}',$$

where A is the horizontal area of the basin and H is the Heaviside step function, satisfying $H(y) = 0$ for $y < 0$, ½ for $y = 0$; 1 for $y > 0$ (Winters et al. 1995). For the case with bottom topography, a similar definition can apply; see the appendix.

Lorenz (1955) first introduced a quasigeostrophic (QG) approximation form of APE for the atmospheric circulation. His definition has since been extended to studies of oceanic circulation (Bryan and Lewis 1979; Oort et al. 1989). In these studies of oceanic circulation, the exact definitions of APE and its source have been replaced by the following approximations:

$$E_a = -\frac{g}{2} \iiint_V (\rho - \overline{\rho})^2 \left(\frac{\partial \overline{\rho}_\theta}{\partial z} \right)^{-1} dv. \tag{2}$$

$$\Phi_s = -g \iiint_V (\rho - \overline{\rho}) \dot{\rho} \left(\frac{\partial \overline{\rho}_\theta}{\partial z} \right)^{-1} dv. \tag{3}$$

Since these definitions are based on the quasigeostrophic approximation, their application to basin-scale circulation may lead to erroneous results. Assuming a linear equation of state and a constant mixing coefficient, the main purpose of his note is to reexamine the classic definition of APE and assess the possible pitfalls of using the QG approximation of APE.

Paralleling the analysis by Winters et al. (1995), the time evolution of APE can be derived as follows. The equations of motion for a Boussinesq fluid are

$$\rho_0 \left(\frac{\partial}{\partial t} \mathbf{u} + \mathbf{u} \cdot \nabla \mathbf{u} + \mathbf{k} f \times \mathbf{u} \right) = -\nabla p + \rho g \mathbf{k} + \nabla \cdot \boldsymbol{\tau}, \tag{4}$$

$$\frac{\partial}{\partial t} \rho + \mathbf{u} \cdot \nabla \rho = \kappa \nabla^2 \rho + \mathrm{CV}, \tag{5}$$

*Woods Hole Oceanographic Institution Contribution Number 9135.

Corresponding author address: Dr. Rui Xin Huang, Department of Physical Oceanography, Woods Hole Oceanographic Institution, Woods Hole, MA 02543.
E-mail: rhuang@whoi.edu

$$\nabla\cdot\mathbf{u} = 0, \tag{6}$$

where ρ_0 is the reference density and $\boldsymbol{\tau}$ is the viscous stress tensor; CV indicates the convective contribution, which cannot be parameterized in terms of a constant mixing rate. We will confine our discussion to an ocean of fixed volume V.

The time rate of change of potential energy in the physical state is

$$\begin{aligned}\frac{d}{dt}E_p &= g\iiint_V z\frac{\partial\rho}{\partial t}\,d\upsilon \\ &= -\iint_S gz\rho\mathbf{u}\cdot\mathbf{n}\,dS - \Phi_{\text{pk}} \\ &\quad + \kappa g\iint_S z\nabla\rho\cdot\mathbf{n}\,dS + \Phi_{\text{me}} - \Phi^p_{\text{CV}},\end{aligned} \tag{7}$$

where

$$\Phi_{\text{pk}} = -\iiint_V g\rho w\,d\upsilon \tag{8}$$

is the rate of conversion from potential to kinetic energy,

$$\Phi_{\text{me}} = \kappa g\iint(\rho_b - \rho_s)\,dx\,dy \tag{9}$$

is the rate of potential energy increase due to mixing supported by the mechanical energy source, and ρ_b and ρ_s are density at the bottom and the upper surface. The density structure in the ocean is maintained by the competition between advection and diffusion. Since vertical advection tends to bring cold and dense water upward in the ocean interior, energy is required to support downward diffusion of warm and light water. For each water parcel mixing raises the center of mass, so the amount of external mechanical energy required is $\varepsilon = -g\kappa\rho_z$. The vertical integration of this relation leads to $g\kappa(\rho_b - \rho_s)$. Thus, Φ_{me} is the total amount of mechanical energy required to support the basic stratification in the ocean. As will be shown shortly, Φ_{me} is one of the most important contributors to circulation energy; Φ^p_{CV} is the energy loss due to convection.

Transferring to density coordinates (x, y, ρ), we have

$$\begin{aligned}\dot{Z}(x, y, z, t) &= \frac{1}{A}\iiint\delta[\rho(\mathbf{x}', t) - \rho(\mathbf{x}, t)] \\ &\qquad\times[\dot{\rho}(\mathbf{x}', t) - \dot{\rho}(\mathbf{x}, t)]\,d\mathbf{x}' \\ &= U(\rho, t) - \dot{\rho}(x, y, \rho, t)D(\rho, t),\end{aligned} \tag{10}$$

where

$$D(\rho, t) = \frac{1}{A}\iint J(x', y', \rho, t)\,dx'\,dy',$$

$$U(\rho, t) = \frac{1}{A}\iint J(x', y', \rho, t)\dot{\rho}(x', y', \rho, t)\,dx'\,dy',$$

where J is the Jacobian of coordinate transformation. For the details, see the appendix. Multiplying (10) by ρ and integrating over the whole volume, we obtain

$$\iiint\rho\dot{Z}(x, y, \rho, t)J(x, y, \rho, t)\,d\rho\,dx\,dy = 0. \tag{11}$$

Thus, the time rate of change of potential energy in the reference state is

$$\begin{aligned}\frac{d}{dt}E_r &= -g\iint_S\mathbf{u}\left(\int^\rho Z(\rho')\,d\rho'\right)\cdot\mathbf{n}\,dS \\ &\quad + \kappa g\iint_S Z\nabla\rho\cdot\mathbf{n}\,dS + \Phi_{\text{mr}} + \Phi^r_{\text{CV}},\end{aligned} \tag{12}$$

where

$$\Phi_{\text{mr}} = \kappa g\iiint_V\left(-\frac{dZ}{d\rho}\right)|\nabla\rho|^2\,d\upsilon > 0 \tag{13}$$

is the rate of potential energy increase in the reference state due to mixing and Φ^r_{CV} is the potential energy change in the reference state due to convection. In general, the vertical mixing rate κ_v and the horizontal mixing rate κ_h are different, so the increase in potential energy in the reference state is defined in terms of

$$\begin{aligned}\Phi_{\text{mr}} &= g\kappa_v\iiint_V\left(-\frac{dZ}{d\rho}\right)\left(\frac{\partial\rho}{\partial z}\right)^2 d\upsilon \\ &\quad + g\kappa_h\iiint_V\left(-\frac{dZ}{d\rho}\right)\left[\left(\frac{\partial\rho}{\partial x}\right)^2 + \left(\frac{\partial\rho}{\partial x}\right)^2\right]d\upsilon,\end{aligned} \tag{14}$$

where the first term is the potential energy increase in the reference state due to vertical mixing in the physical state, while the second term is due to horizontal mixing.

The time rate of change of APE is the difference between the time rate of change of E_p and E_r; thus,

$$\begin{aligned}\frac{d}{dt}E_a &= \Phi_s + \Phi_{\text{me}} - \Phi_{\text{mr}} - \Phi_{\text{pk}} \\ &\quad - g\iint_S\left[z\rho - \int^\rho Z(\rho')\,d\rho'\right]\mathbf{u}\cdot\mathbf{n}\,dS - \Phi_{\text{CV}},\end{aligned} \tag{15}$$

where

$$\Phi_s = \kappa g \iint_S (z - Z)\nabla\rho\cdot\mathbf{n}\, dS$$

$$= g \iint B(H - Z)\, dx\, dy \qquad (16)$$

is the source of APE due to surface buoyancy flux

$$B = \kappa \left.\frac{d\rho}{dz}\right|_{z=H}.$$

For a system without mass exchange through the surface, the fifth term on the right-hand side of (15) vanishes, so the APE balance for an equilibrium state is

$$\frac{d}{dt}E_a = \Phi_s + \Phi_{\text{me}} - \Phi_{\text{mr}} - \Phi_{\text{pk}} - \Phi_{\text{CV}} = 0. \qquad (17)$$

Therefore, the generation of APE due to surface buoyancy flux and mixing driven by an external energy source is balanced by an increase of potential energy in the reference state, conversion to kinetic energy, and energy loss due to convective mixing.

The mixing rate during convective overturning is difficult to define exactly. As will be shown in section 3, it is more convenient to calculate the net sum of $\Phi_s' = \Phi_s - \Phi_{\text{CV}}$, so the balance of APE is

$$\frac{d}{dt}E_a = \Phi_s' + \Phi_{\text{me}} - \Phi_{\text{mr}} - \Phi_{\text{pk}} = 0. \qquad (17')$$

In comparison, the time rate of change of potential energy in a steady state is

$$\frac{d}{dt}E_p = \Phi_s^p + \Phi_{\text{me}} - \Phi_{\text{pk}} - \Phi_{\text{CV}}^p = 0. \qquad (18)$$

Note that in the steady-state surface thermal forcing cannot create potential energy

$$\Phi_s^p = g \iint BH\, dx\, dy = 0.$$

Although this seems like a shocking conclusion, it is a logical consequence of the assumption of incompressibility made in the model. Since we assume that the fluid is incompressible, there is no direct link between the change in internal energy due to heating/cooling and potential energy. Therefore, thermal forcing on the surface cannot create potential energy directly, and the potential energy balance is reduced to

$$\frac{d}{dt}E_p = \Phi_{\text{me}} - \Phi_{\text{pk}} - \Phi_{\text{CV}}^p = 0. \qquad (18')$$

In the present case of no wind stress input, the only source of potential energy is the mechanical energy supporting mixing, and this is used for supporting the energy required for sustaining momentum dissipation and convection.

According to (16), in contrast, thermal forcing can create APE. This apparent contradiction is due to the fact that APE is defined as a global quantity, and the APE source/sink is meaningful only when it is linked to the global structure.

Both Eqs. (15) and (17) include the available potential energy source term due to mixing driven by the mechanical energy source. In comparison, in the QG approximation of APE and its sources, the background stratification is assumed to be given. Consequently, the term representing the mechanical energy source required for mixing does not exist in the corresponding balance equation for the time evolution of available potential energy derived from the QG approximation. Therefore, the important dynamic role of mixing in setting up the basic stratification and supporting the available potential energy for oceanic circulation cannot be clearly explained using the QG approximation of APE.

Furthermore, even the available potential energy source due to surface thermohaline forcing is not accurately represented in the QG approximation. The ocean is thermally forced from the upper surface, but the surface heat flux, such as solar radiation, can penetrate only a few meters. Heat does penetrate into the deep ocean, but this is due to mixing sustained by a source of mechanical energy. Because the energy of mixing is represented by the Φ_{me} term in (17), the contribution of heating itself will be confined to the surface layer. Since $z - Z \approx H - Z$ in (16) is always positive, heating at the upper boundary would generally reduce the APE, but cooling at the upper boundary would increase APE.

However, the results obtained from the QG approximation for the source of APE are quite different, as will be shown in section 3. The errors resulting from applying the QG approximations come from several steps involved. From the exact definition (1), one can write

$$E_a = \iint_A C(x, y)\, dx\, dy,$$

$$C(x, y) = g \int_{H_b}^{H_s} (z - Z)\, dz. \qquad (19)$$

Integration by parts plus some manipulations lead to

$$C(x, y) = -\frac{g}{2}\int_{\rho_b}^{\rho_s} (z - Z)^2\, d\rho - g\int_{\rho_b}^{\rho_s} Z\left(z - \frac{Z}{2}\right) d\rho + \frac{g}{2}\int_{\rho_{\max}}^{\rho_{\min}} Z^2\, d\rho + \frac{g}{2}[H_s^2(\rho_s - \rho_{\min}) - H_b^2(\rho_b - \rho_{\max})], \qquad (20)$$

where $\rho_s = \rho_s(x, y)$ and $\rho_b = \rho_b(x, y)$; $\rho_{\max}$ and $\rho_{\min}$ are the global density maximum and minimum. If we omit the second, third, and fourth terms on the right-hand side of (20) and approximate the first term on the right-hand side by substituting the global mean height over

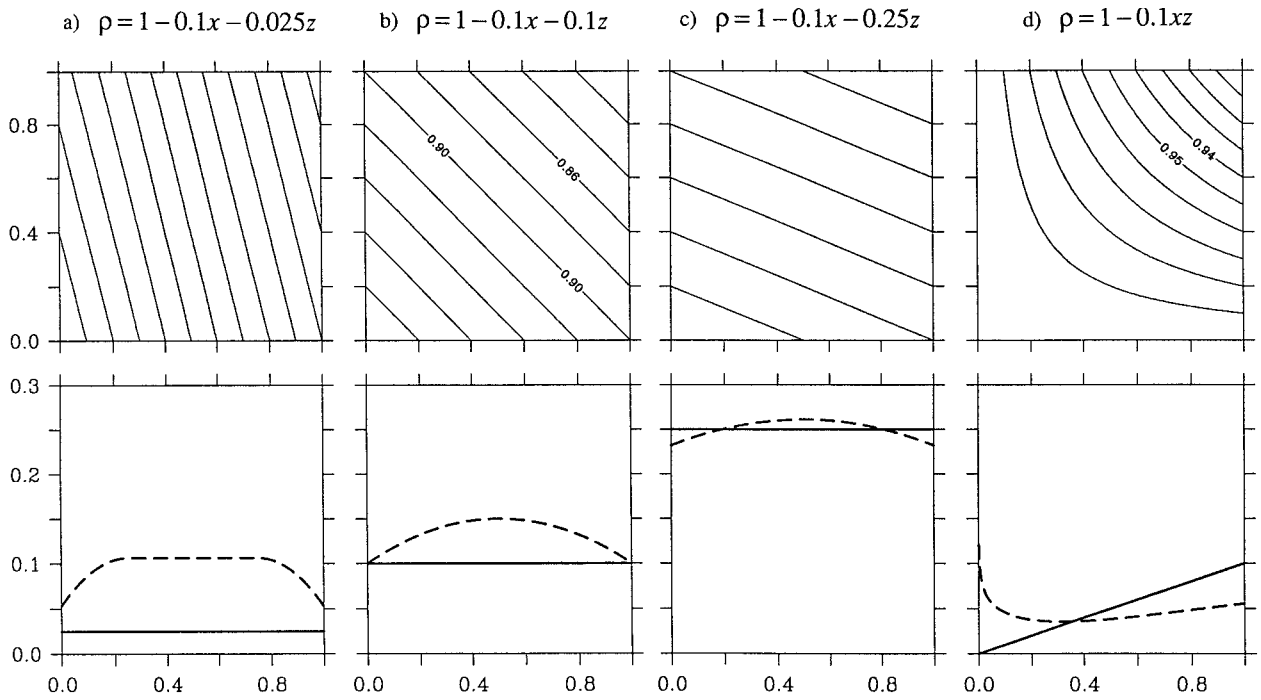

FIG. 1. Density distribution and potential energy sources. The upper panels show the density distribution, and the lower panels show the potential energy source due to mixing in the physical state (solid line) and in the reference state (dashed line).

a constant density surface $\tilde{z}(\rho)$ for the reference surface $Z(\rho)$, using z as the vertical coordinate and assuming the Jacobian is approximately equal to $\partial\tilde{\rho}/\partial z$, we are left with the QG approximation, (2). The errors introduced in these approximations will be discussed shortly.

2. Two-dimensional examples

Assume a density distribution $\rho = \rho_0(1 - \alpha xz)$, where $\rho_0 = 29.0$ and $\alpha = 4/29$, x and z are the nondimensional coordinates. The APE for this system can be calculated analytically (the algebra is rather elementary and tedious, so it is not included here):

$$E_a = \frac{\alpha}{54} g\rho_0, \qquad E_{QG} = \frac{\alpha}{36} g\rho_0. \tag{21}$$

Thus, the QG approximation of APE is 50% larger than the exact APE.

Integrating (19) over the region of [0,1] leads to an exact balance

$$\frac{1}{54}\alpha g\rho_0 = \left(\frac{403}{5184} + \frac{29}{5184} - \frac{17}{54} + \frac{1}{4}\right)\alpha g\rho_0. \tag{22}$$

Clearly, neglecting the second, third, and fourth terms in (20) and replacing the first term $\iint (z - Z)^2\, d\rho\, dx$ with

$$\int\int \frac{(\rho - \tilde{\rho})^2}{\tilde{\rho}_z}\, dz\, dx$$

can introduce large errors.

As discussed above, mixing light water downward increases the potential energy of the system, as indicated by the Φ_{me} term; however, mixing can also increase potential energy in the reference state, and thus reduce APE, as indicated by the Φ_{mr} term. Whether mixing is a net source or sink of APE depends on the slope of the isopycnals and the relative strength of vertical and horizontal mixing. As an example, we study two cases with simple stratification distribution. Using (9) and (14) the rate of potential energy change due to mixing in both the physical and reference state can be calculated analytically. (Here again, since such calculations are rather elementary and tedious, they are excluded from the text.) For simplicity, the horizontal and vertical mixing coefficients, κ_v and κ_h, are assumed to obey the relation $\kappa_v/H^2 = \kappa_h/L^2$, where H and L are the depth and horizontal width of the model basin.

When the slope of the isopycnal is steep, horizontal mixing dominates, so the increase of potential energy in the reference state is larger than that in the physical state, resulting in a net loss of available potential energy (Fig. 1a). As the vertical density gradient increases, potential energy increases in both the physical and the reference state, and there can be a net APE source due to mixing (Figs. 1b and 1c). (For large-scale circulation in the oceans, mixing can be more conveniently defined in terms of isopycnal and diapycnal mixing. By projecting the isopycnal and diapycnal mixing onto the vertical and horizontal di-

rection, our argument still applies. However, the spatial inhomogeneity of mixing should be taken into consideration carefully.)

In a more realistic stratification, $\rho = 1 - 0.1xz$, there is a net source of APE in the right-hand side of the model because the vertical stratification is strong, while the horizontal density gradient is relatively weak. On the other hand, the source of potential energy in the physical state due to vertical mixing approaches zero toward the left edge of the model, but the source of potential energy in the reference state becomes unbounded toward the left edge because of the extremely strong horizontal density gradient. The distribution of the potential energy source due to mixing in the physical and reference state in this case is a typical example of basin-scale circulation, as will be explained in detail shortly.

3. Results from a three-dimensional numerical model

Numerical experiments has been carried out using a three-dimensional primitive equation model by Cox (1984). The model ocean is a $60° \times 60°$ square basin, with a constant depth of 5.7 km. The horizontal resolution is $4° \times 4°$, and there are 15 layers vertically, with the top layer 30 m thick. The model is driven by a relaxation boundary condition for temperature only, with a reference temperature that is 25°C at the equator and decreases linearly to 0°C at the northern boundary. A simplified equation of state is used:

$$\rho = 0.7948S_o - 0.05968T - 0.0063T^2 + 3.7315 \times 10^{-5}\, T^3. \quad (23)$$

Since the equation of state is nonlinear, the cabling effect induces additional terms in the APE balance equation. However, their net contribution to the APE is rather small, so we will treat them as part of the horizontal mixing term.

There is neither wind stress nor freshwater forcing in the model. The coefficients of horizontal momentum dissipation and of tracer mixing are $A_h = 2.5 \times 10^5$ m^2 s^{-1} and $\kappa_h = 10^3$ m^2 s^{-1}, respectively; the vertical momentum dissipation coefficient is $A_v = 10^{-4}$ m^2 s^{-1}. The vertical tracer mixing coefficient is $\kappa_v = 10^{-4}$ m^2 s^{-1} in the first experiment, but it will be changed to 10^{-5} m^2 s^{-1} and 10^{-3} m^2 s^{-1} for two additional experiments to be discussed shortly. The numerical model includes a scheme of complete convective adjustment, so that stratification is always stable in each water column. The model is started from an initial state of a homogeneous ocean with no motion and integrated for 6000 years to guarantee that the quasi-steady state has been approached. The strength of the time mean meridional overturning is about 9.1 Sv (Sv $\equiv 10^6$ m^3 s^{-1}).

In the present case, the APE source term due to surface thermal forcing is slightly modified by absorbing the energy loss through convection. Cooling at the surface creates dense water on the top of the ocean and sinking of dense water provides the source of APE. However, a major part of APE generated by cooling is lost through strong small-scale mixing and turbulence in the process of convective adjustment. (Our calculations indicated that about 30% of the APE generated by cooling at the surface was lost through convective adjustment.) Without considering this loss of APE, $\Phi_{\rm CV}$, one cannot obtain a balanced budget of the APE sources and sinks. A simple way to consider the net APE source due to thermal forcing and convection is to use the center of the completely convective water column, $h_{m/2}$, as the height in the physical state, so the modified source term due to surface thermal forcing is

$$\Phi_s' = \kappa_v g \iint_S (z - Z)\nabla\rho\cdot\mathbf{n}\, dS - \Phi_{\rm CV} = g \iint B(h_{m/2} - Z)\, dx\, dy. \quad (24)$$

Our analysis here is based on results from a finite-difference grid of $15 \times 15 \times 15$; thus, we rewrite the APE balance (17′) in terms of

$$\frac{d}{dt}E_a = \sum_1^{15} (\phi_s'^i + \phi^i_{\rm me} - \phi^i_{\rm mr} - \phi^i_{\rm pk}) = 0, \quad (17'')$$

where $\phi_s'^i$, $\phi^i_{\rm me}$, $\phi^i_{\rm mr}$, and $\phi^i_{\rm pk}$ are the corresponding source and sink terms defined for the ith latitude band of grid boxes.

The heat loss to the atmosphere reaches its maximum (60 W m^{-2}) in the middle of the western boundary. However, this local feature does not appear as a maximum on the map of APE sources. Instead, the region of strong source of APE is located much farther poleward because the depth factor $h_{m/2} - Z$ dominates the strength of the APE source, as indicated in (24) (Fig. 2). Although there is strong heat flux into the ocean along the equatorial edge of the basin, its contribution to APE is rather small because $h_{m/2} - Z$ is very small near the equator.

For comparison, the source of APE due to surface forcing based on the QG approximation (3) indicates a strong source of APE in the equatorial region (the thin curve labeled $\phi_{s,\rm QG}$ in Fig. 2), similar to the results of Oort et al. (1994, their Fig. 5c). According to such a definition, most of the APE would be generated near the equator instead of in the polar basin. This seems to be in contradiction to the real physical process happening in the ocean where potential energy is released when dense water sinks into the deep ocean.

Most importantly, the exact definition of the source of APE includes the contribution due to mixing driven by the mechanical energy source, as indicated by the dashed line in Fig. 2. As is well known, mixing raises the center of mass against gravity, so mixing requires

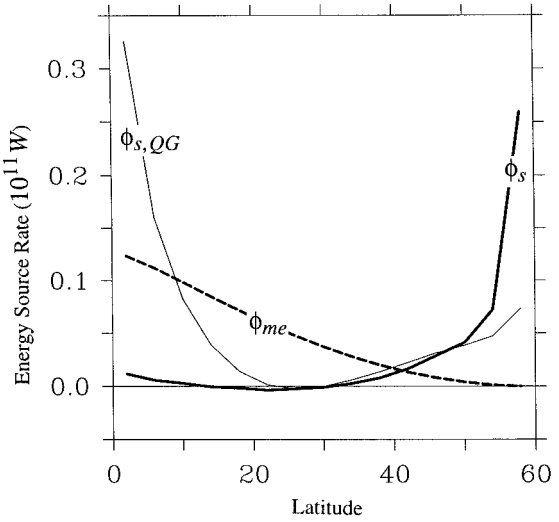

FIG. 2. APE sources (integrated over each 4° latitude band) due to surface forcing and interior mixing: ϕ_s is the APE source due to surface forcing based on the exact denifition, $\phi_{s,QG}$ is the APE source due to surface forcing under the QG approximation, and ϕ_{me} is the APE source due to external mechanical energy sustaining vertical mixing.

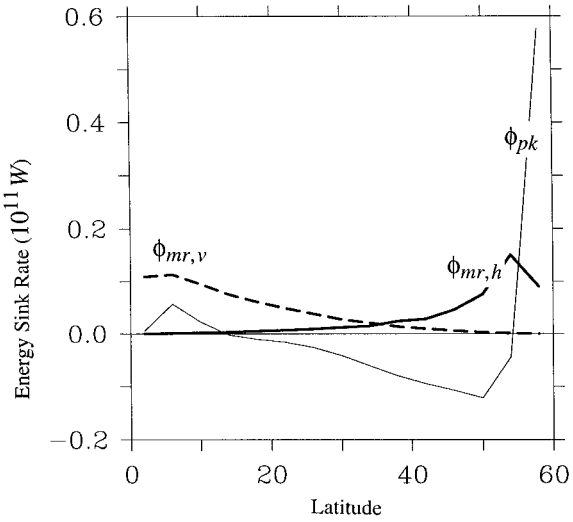

FIG. 3. APE sinks (integrated over each 4° latitude band): $\phi_{mn,v}$ is due to vertical mixing, $\phi_{mr,h}$ is due to horizontal mixing, and ϕ_{pk} is the rate that potential energy is converted to kinetic energy.

an external source of mechanical energy. Since mixing is essential in setting up vertical stratification and circulation in the ocean, external energy supporting mixing is of vital importance for the oceanic circulation. In the equatorial part of the basin, stratification is strong, so the external energy source supporting mixing is also very strong (Fig. 2).

In a steady state, APE sources are exactly balanced by sinks, including the increase of potential energy in the reference state due to both vertical and horizontal mixing in the physical state and conversion to kinetic energy. The sink of APE due to vertical mixing is strong in the southern part of the basin, while the sink due to horizontal mixing is strong in the poleward part of the basin, as indicated by the heavy solid line and the heavy dashed line in Fig. 3. (However, the horizontal distribution of mixing energy in the real oceans may be different because the rate of diapycnal mixing is highly inhomogeneous in space.) The conversion rate to total kinetic energy can be rewritten in terms of the deviation of density from the basin mean, $-\int (\rho - \overline{\rho})w\, dv$. Accordingly, most of the APE-to-TKE conversion takes place along the northern edge of the basin, where density is highest and sinking takes place.

Combining Figs. 2 and 3, we obtain the latitudinal distribution of source (thermal forcing plus mixing) and sink (mixing and conversion to kinetic energy) of APE (Fig. 4). Accordingly, the major sink of APE is near the northern edge of the basin where water sinks. This sink is partially balanced by the local source of APE due to thermal forcing, and the rest is supplemented by the net source of APE at low and middle latitudes.

The global balance of APE and TKE is shown in Fig. 5, where results from three numerical experiments are included, with $\kappa_v = 10^{-5}$, 10^{-4}, 10^{-3} m^2 s^{-1}. (For the case of $\kappa_v = 10^{-5}$ m^2 s^{-1}, the model is run for 14 000 years in order to reach a true equilibrium). Note that these three experiments were all carried out under the identical relaxation condition for temperature, with the only difference being in the vertical tracer mixing parameter. As κ_v increases ten

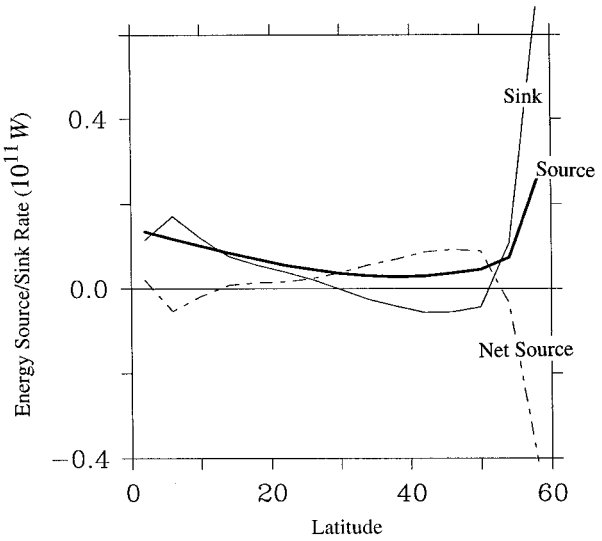

FIG. 4. APE sources and sinks (integrated over each 4° latitude band) due to surface forcing and interior mixing, and energy conversion.

$a)\kappa = 10^{-5}\, m^2 s^{-1}$, MOR = 1.68 *Sv*, PHF = 0.099 *PW* ($472\times10^{-6}\, W\, m^{-3}$)

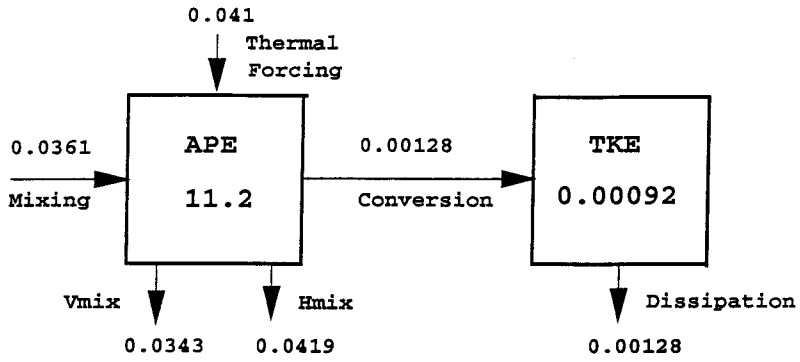

$b)\kappa = 10^{-4}\, m^2 s^{-1}$, MOR = 9.1 *Sv*, PHF = 0.362 *PW* ($1726\times10^{-6}\, W\, m^{-3}$)

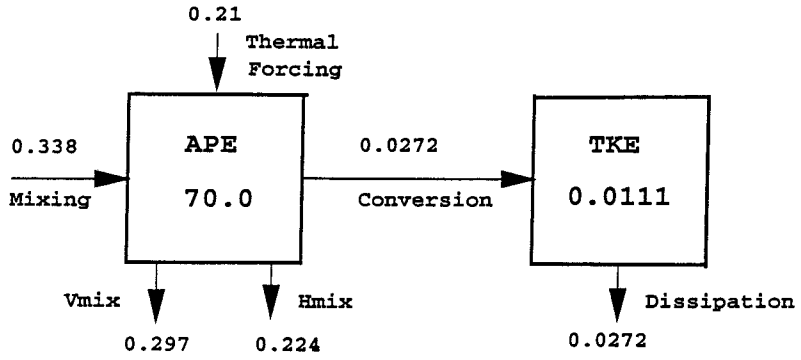

$c)\kappa = 10^{-3}\, m^2 s^{-1}$, MOR = 33.27 *Sv*, PHF = 1.131 *PW* ($5391\times10^{-6}\, W\, m^{-3}$)

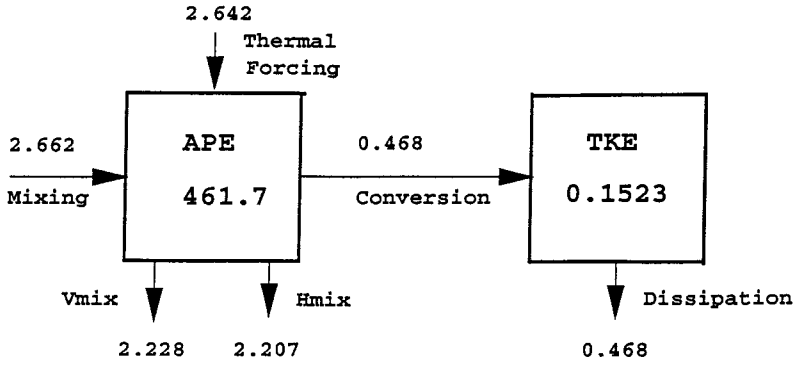

FIG. 5. Balance of APE and TKE (total kinetic energy) for three cases with $\kappa_v = 10^{-5}$, 10^{-4}, 10^{-3} m^2 s^{-1}. MOR is the meridional overturning rate, in 10^6 m^3 s^{-1}; PHF is the poleward heat flux in 10^{15} W; Vmix and Hmix indicate the potential energy increase in the reference state due to vertical and horizontal mixing. Both APE and TKE are in units of joules per cubic meter, while all flux terms are in units of 10^{-6} W m^{-3}.

times, all quantities increase about ten times, including the total amount of APE and TKE, and all fluxes. Although the dependence of the meridional overturning rate, poleward heat flux, and some other fluxes on the vertical diffusivity has been studied by many investigators, for example, F. Bryan (1987), the dynamic role of mechanical energy supporting vertical (diapycnal) mixing has not been discussed previously. This is our focus here.

In all three cases the source of APE due to mixing driven by an external energy source is about the same as the source of APE due to surface thermal forcing. Thermal forcing alone cannot determine the strength of the APE source due to surface forcing, the total amount of APE, the strength of meridional overturning rate (MOR), and the poleward heat flux (PHF). In contrast, under a given surface thermal forcing condition, the amount of energy available for mixing controls the stratification and thus the meridional pressure gradient, which in turn controls the strength of meridional overturning, the poleward heat flux, and even the APE source rate due to surface thermal forcing.

For example, when $\kappa_v = 10^{-4}$ m^2 s^{-1}, the external energy required for sustaining the mixing is about 0.338×10^{-6} W m^{-3}, which is larger than the APE source due to surface thermal forcing of 0.21×10^{-6} W m^{-3}. The net APE source due to mixing is equal to the sum of the APE source of mixing, sustained by external energy, minus the potential energy increase in the reference state due to mixing in the physical state, so it is 0.183×10^{-6} W m$^{-3} < 0$. However, it would be a mistake to ignore the source of mechanical energy required to sustain mixing and claim that mixing only dissipates APE. As discussed above, the mechanical energy to sustain mixing contributes about half of the APE source. In addition, mixing driven by the external energy source also controls the strength of the APE source due to surface thermal forcing. Furthermore, the actual amount of external energy required for sustaining the mixing is about 10 times larger than the value of 0.338×10^{-6} W m^{-3} because the efficiency of mixing is only about 10%, as suggested by Osborn (1980). This large amount of energy required for mixing may come from tidal dissipation, internal wave breaking, or wind stress input, but details of this energy source are left for further study.

In many existing textbooks and papers, the oceanic circulation has been compared with other heat engines. However, there is a big difference between oceanic circulation and other heat engines. As shown above, in order to put the oceanic engine in motion, the mechanical energy required for sustaining the background mixing is much larger than the amount of energy converted from potential energy to kinetic energy. The ratio is about 10. If we consider the efficiency of 10% suggested by Osborn (1980), this energy ratio will be on the order of 100.

The exact sources for the mechanical energy to support mixing may vary for different oceans or model oceans. Mixing requires mechanical energy of very small scale, most likely from small-scale internal waves and turbulence. Because most strong currents in the oceans are surface-intensified, kinetic energy of large-scale currents may not be a major source of mixing for the oceans. On the other hand, external mechanical energy, such as tidal mixing and wind stirring, may be more likely major sources of mechanical energy to sustain mixing. Although strong mixing near the Antarctic Circumpolar Current (ACC) may be due to lee waves generated over the large-scale topography, the ACC itself is strongly affected by the wind stress input, so mixing there is also driven indirectly by external mechanical energy.

Thus, within the region of realistic parameters, the oceanic circulation is not a heat engine! However, there is a special region where very weak molecular diffusion, on the order of 10^{-8} m^2 s^{-1}, can alone drive the oceanic circulation. Since the diffusivity is about 1000 times smaller than in case a (Fig. 5), the meridional overturning rate and poleward heat flux will be reduced to about 0.1 Sv and 0.01 PW. This region is, of course, only an idealized case existing in theory, and it is totally unrelated to the real oceans.

This study is focused on a few numerical experiments for thermally driven circulations in a Boussinesq fluid. The partition of the APE source between buoyancy forcing and mechanical mixing may vary with the forcing and parameters used in the models. In addition, one of the most important simplifications is that we exclude the role of wind stress. Including wind stress is likely to change the direction of energy conversion between potential and kinetic energy. In many cases with wind forcing, kinetic energy generated through wind stress forcing is partially transformed to potential energy, for example, Holland (1975), Böning (1989), and Treguier (1992).

4. Conclusions

We have analyzed the energetics of the oceanic circulation based on the concept of available potential energy, especially the dynamic role of mechanical energy in sustaining mixing and thus the basic stratification and meridional thermohaline circulation. In particular, the mechanical energy that sustains mixing contributes a substantial part (in our experiments it is about half) of the APE directly and it also controls the APE source due to surface thermal forcing. The QG approximation of APE and its source is based on a simple extension from Lorenz's (1955) definition for atmospheric circulation. Such a simple definition may not be appropriate for the study of oceanic circulation because it neglects the important contribution due to the source of mechanical energy required to sustain mixing. In addition, such a definition may give an incorrect APE source distribution due to surface thermal forcing.

Although our discussion here is primarily about APE, the mixing energy argument should apply to the potential energy balance as well. Namely, the mechanical energy

required to sustain vertical mixing is an essential part of the oceanic energy balance. Although such a term is included in a few papers and books (e.g., Holland 1975), so far there are no estimates for such a term in an energy budget for either numerical models or real oceans.

The application of the exact definition of APE and its sources and sinks to the real oceans remains a challenge at this time. The major difficulties are the nonlinear equation of state, including the effects of salinity and pressure, the nonuniqueness of the potential density surface, and above all the highly nonuniform distribution of tracer mixing and the uncertainty of the thermohaline forcing (especially in the polar oceans where most of the APE sources are located.)

Although there exists no analytical expression of APE for the real oceans at this time, it is possible to define both APE and its source due to surface thermohaline forcing by a computer-sorting program. The essence of such a sorting program is the following: the ocean is divided into many small grid boxes, each of which is represented by its average temperature and salinity. Assuming there is no bottom topography, water masses in all these grid boxes are sorted out and stacked up in the reference state, using the sea surface as a reference level. Using a single reference level is, of course, not enough to guarantee the stability at deep levels. Thus, all water parcels in the reference state beneath a certain level are resorted, using a new reference level slightly below the sea surface. This resorting process can be repeated, and by using very fine reference intervals the final reference state with minimum potential energy can be calculated to any given degree of accuracy. The case with bottom topography can be handled with additional iterations. Since solving such a problem involves exact definitions of APE and its source/sink, requiring elaborate derivation and long calculations, this will be discussed in a separate study.

Acknowledgments. I have benefited from many discussions with Xiang Ze Jin, Joe Pedlosky, Roger Samelson, and Kraig Winters. This study was supported by NASA through Grant NAGW-4331 and the National Science Foundation through Grant OCE93-00706 to the Woods Hole Oceanographic Institution.

APPENDIX

APE for Oceans with Topography

Due to the existence of separate deep basins the case with bottom topography may allow multiple solutions of the reference state that have local minimum potential energy in the phase space. For simplicity, our discussion here is limited to the solution that has the global minimum potential energy. For a given basin, the topography can be defined by specifying the horizontal area as a function of the geometric height

$$A = A(z) \quad \text{for} \quad 0 \le z \le h,$$

where $z = h$ is the sea surface. The total volume of the basin at a given level z is a given function of z

$$v(z) = \int_0^z A(z')\, dz'.$$

Accordingly, given the total volume above the bottom, the corresponding vertical coordinates can be found through the inverse function $z = z(v)$.

Thus, the vertical coordinate in the reference state can be defined as

$$Z(\mathbf{x}, t) = Z(v), \quad \text{with}$$

$$v = \iiint_V H(\rho(\mathbf{x}', t) - \rho(\mathbf{x}, t))\, d\mathbf{x}'.$$

The time rate of change of the reference level can be calculated by transformation to density coordinates (x, y, ρ), with the Jacobean $J(x, y, \rho, t) = \partial(x, y, z)/\partial(x, y, \rho)$ defined in the physical state, and the overdot indicating the time rate:

$$\begin{aligned}
\dot{Z}(\mathbf{x}, t) &= \frac{1}{A(Z(\rho))} \iiint \frac{\partial}{\partial t} H(\rho(\mathbf{x}', t) - \rho(\mathbf{x}, t))\, d\mathbf{x}' \\
&= \frac{1}{A(Z(\rho))} \iiint \delta[\rho(\mathbf{x}', t) - \rho(\mathbf{x}, t)][\dot{\rho}(\mathbf{x}', t) - \dot{\rho}(\mathbf{x}, t)]\, d\mathbf{x}' \\
&= \frac{1}{A(Z(\rho))} \iint dx'\, dy' \int \delta[\rho(x', y', \rho', t) - \rho(x, y, \rho, t)]\dot{\rho}(x', y', \rho', t) J(x', y', \rho', t)\, d\rho' \\
&\quad - \frac{1}{A(Z(\rho))} \iint dx'\, dy' \int \delta[\rho(x', y', \rho', t) - \rho(x, y, \rho, t)]\dot{\rho}(x, y, \rho, t) J(x', y', \rho', t)\, d\rho' \\
&= \frac{1}{A(Z(\rho))} \iint dx'\, dy'\, \dot{\rho}(x', y', \rho, t) J(x', y', \rho, t) - \frac{1}{A(Z(\rho))} \iint dx'\, dy'\, \dot{\rho}(x, y, \rho, t) J(x', y', \rho, t) \\
&= U(\rho, t) - \dot{\rho}(x, y, \rho, t) D(\rho, t),
\end{aligned} \tag{A1}$$

where

$$D(\rho, t) = \frac{1}{A(Z(\rho))} \iint J(x', y', \rho, t)\, dx'\, dy', \tag{A2}$$

$$U(\rho, t) = \frac{1}{A(Z(\rho))} \iint J(x', y', \rho, t)\dot{\rho}(x', y', \rho, t)\, dx'\, dy', \tag{A3}$$

where $-D(\rho, t)$ and $-U(\rho, t)$ indicate the average isopycnal layer thickness and time rate term, noting that $-J$ is the local isopycnal layer thickness. Using these relations, the integration of density multiplied by the time rate term is

$$\begin{aligned}
&\iiint \rho\dot{Z}(x, y, \rho, t)J(x, y, \rho, t)\, d\rho\, dx\, dy \\
&\quad = \int d\rho \left(\rho U(\rho, t) \iint J(x, y, \rho, t)\, dx\, dy\right) \\
&\qquad - \int d\rho \left(\rho D(\rho, t) \iint \dot{\rho}(x, y, \rho, t) \right. \\
&\qquad\qquad \left. \times J(x, y, \rho, t)\, dx\, dy\right) \\
&\quad = \int d\rho \left(A(Z(\rho))\rho U(\rho, t)D(\rho, t)\right) \\
&\qquad - \int d\rho \left(A(Z(\rho))\rho D(\rho, t)U(\rho, t)\right) = 0.
\end{aligned}$$

Thus, (11) is valid for the case with topography.

REFERENCES

Böning, C., 1989: Influence of a rough bottom topography on flow kinematics in an eddy-resolving circulation model. *J. Phys. Oceanogr.,* **19,** 77–97.

Bryan, F., 1987: Parameter sensitivity of primitive equation ocean general circulation models. *J. Phys. Oceanogr.,* **17,** 970–985.

Bryan, K., and L. J. Lewis, 1979: A water mass model of the world ocean. *J. Geophys. Res.,* **84,** 2503–2517.

Cox, M. D., 1984: A primitive equation, 3-dimensional model of the ocean. GFDL Ocean Group Tech. Rep. No. **1**. [Available from GFDL/Princeton University, Princeton, NJ 08542.]

Holland, W. R., 1975: Energetics of baroclinic oceans. *Numerical Models of Ocean Circulation,* National Academy of Sciences Press, 168–177.

Lorenz, E. N., 1955: Available potential energy and the maintenance of the general circulation. *Tellus,* **7,** 157–167.

Oort, A. H., S. C. Ascher, S. Levitus, and J. P. Peixoto, 1989: New estimates of the available potential energy in the world ocean. *J. Geophys. Res.,* **94,** 3187–3200.

——, L. A. Anderson, and J. P. Peixoto, 1994: Estimates of the energy cycle of the oceans. *J. Geophys. Res.,* **99,** 7665–7688.

Osborn, T. R., 1980: Estimates of the local rate of diffusion from dissipation measurements. *J. Phys. Oceanogr.,* **10,** 83–89.

Trequier, A. M., 1992: Kinetic energy analysis of an eddy resolving, primitive equation model of the North Atlantic. *J. Geophys. Res.,* **97,** 687–701.

Winters, K. B., P. N. Lombard, J. J. Riley, and E. A. D'Asaro, 1995: Available potential energy and mixing in density-stratified fluids. *J. Fluid Mech.,* **289,** 115–128.